KURENAI
Kyoto University Research Information Repository

KYOTO UNIVERSITY

Title	Secondary-ion emission from HEN semiconductive materials under MeV-energy heavy-ion bombardment
Author(s)	Ninomiya, S; Imada, C; Nagai, M; Nakata, Y; Imanishi, N
Citation	PHYSICAL REVIEW A (2004), 70(4)
Issue Date	2004-10
URL	http://hdl.handle.net/2433/50205
Right	Copyright 2004 American Physical Society
Type	Journal Article
Textversion	publisher; none

Kyoto University

Secondary-ion emission from III-V semiconductive materials under MeV-energy heavy-ion bombardment

Satoshi Ninomiya, Chikage Imada, Masafumi Nagai, Yoshihiko Nakata, and Nobutsugu Imanishi

Department of Nuclear Engineering, Kyoto University, Sakyo, Kyoto 606-8501, Japan

Secondary-ion emission from III-V semiconductive chemical compounds (InP, InAs, and InSb) has been experimentally studied at heavy-ion energies from 0.5 to 5.0 MeV, where electronic collision is a dominant process. Various secondary ions such as large cluster ions and atomic ions were observed. Yields of In atomic and cluster ions depend scantly on the incident energy, and those of group-V atomic ions and of cluster ions containing group-V elements can be expressed by an exponential function of S_e^{-1}, where S_e is the electronic stopping power. This fact shows that the ionization probabilities of the atoms and the clusters whose ionization potentials are higher than the work functions of target materials are increased by transient electronic excitation induced by ion bombardment. The energy distributions of the atomic ions show that the singly charged atomic ions are emitted through the linear collision cascade process even at MeV incident energies, and the multiply charged ions are produced by a projectile-induced simultaneous process of ionization and recoiling of atoms on the target surface. The yield dependences of the cluster ions on the electronic stopping power and on the cluster size are so much different from those for SiO_2. This fact precludes the multiple-bond-breaking process applied to the insulating material. Structural instabilities caused by high-density electronic excitations, which are known to take place in GaAs irradiated by slow multiply charged ions or lasers, are a possible cause of the cluster-ion emission from the semiconductive compounds at the MeV energy range.

I. INTRODUCTION

At MeV energies, the electronic stopping power increases with increasing projectile energy and vice versa for the nuclear stopping power; for example, in the case of 5-MeV Si projectiles the former is 100 times as high as the latter. It has been a great concern since the discovery of emission of large ionized molecules by Torgerson, Skowronski, and Macfarlane how the energy deposited to excitation of an electronic system transfers to kinetic energies enough to sputter large molecules [1]. So far, most experimental works were done for weakly bound materials such as condensed gases and biomolecules [2,3] and only a few works were done for tightly bound chemical compounds [4–10] except for alkali halides [11]. In contrast to nuclear-collision-induced sputtering at low incident energies, the emission mechanism of large molecules is very complex. Several theoretical models were developed. Representatives are Coulomb explosion models [12], thermal spike models [13], electronic shock-wave models [14], and pressure-pulse models [15]. Each model reproduces only a few of experimental results mainly of weakly bound materials. The mechanism of the electronic sputtering depends so much on material properties and is still open especially for tightly bound chemical compounds.

Thus, the aim of the present study is to reveal in detail the material dependence of the mechanism. We have measured yields and energy distributions of secondary ions emitted from In (group-V) semiconductive compounds at incident energies between 0.5 and 5 MeV, where the electronic collision process far dominates over the nuclear one, and have compared them with those of SiO_2 (insulator), Si (semiconductor), and Ga (group-V) semiconductive compounds [4–10]. Systematical dependences on the electric properties

of the materials have been obtained for the emission of singly and multiply charged atomic ions and cluster ions.

II. EXPERIMENT

Mass spectra of secondary ions were measured by using a linear and a reflective time-of-flight (TOF) mass spectrometer. A 0.5–5.0-MeV Si-ion beam extracted from a Kyoto University 1.7-MV tandem Cockcroft-Walton accelerator was guided to a target chamber through a beam line, where the beam was chopped to a width of 50 ns every 100 μs by applying a high-voltage pulse between parallel electrodes. A neutral particle rejecting system, which was composed of four sets of dipole magnets installed in front of the target chamber, successfully rejected neutral particles formed by charge changing collisions with residual gaseous molecules in the beam duct and, as a result, reduced the continuous background produced by the neutral particle incidence on the target. Targets used were the semiconductive chemical compounds of InP, InAs, and InSb, and they were crystalline wafers with high degrees of purity available on the market. The front surface of each target was purified by bombardment with an intense continuous ion beam for 2000 s before each 5000 s data taking. The procedure drastically reduced the intensities of impurity components such as hydrocarbons, sodium, and potassium. Then, the pulsed beam was incident on the target at an angle of 60° with respect to the surface normal, and the resultant secondary ions were extracted with a parallel electrode and detected with a channel electron multiplier set on the axis of the surface normal in the case of the linear TOF mass spectrometer. In the case of the reflective type, they were reflected with a two-composed of 4 and 15 circular electrodes and were detected with another channel
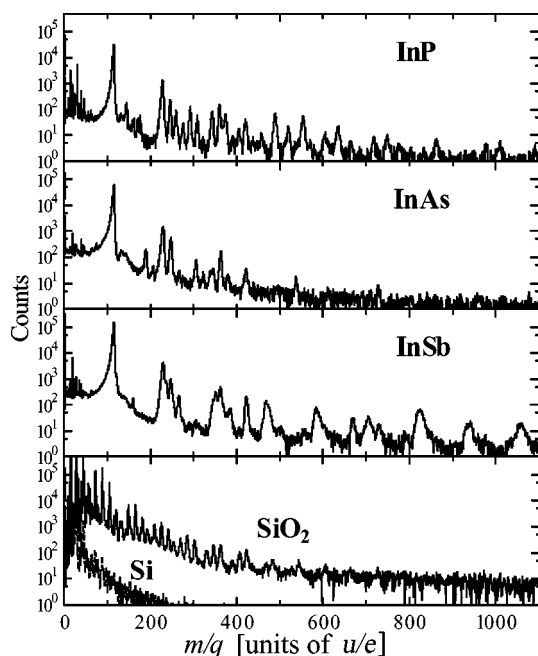
FIG. 1. Mass spectra of secondary ions emitted from the InP, InAs, and InSb targets under 5.0 MeV Si^{3+} bombardment. The secondary ions were measured using the linear time-of-flight spectrometer. Mass spectra of the SiO_2 and Si targets are also shown [4].

electron multiplier. An einzel lens and a deflector were set in a field-free drift region in order to efficiently collect secondary ions. In the present measurement, the detection efficiency of the reflective spectrometer was as high as that for the linear type. The channel electron multipliers had high performances (a counting limit higher than 1×10^8 counts/s and noise less than 0.01 counts/s at an applied voltage of 4 kV) and responded to ions, electrons, soft x rays, and vacuum ultraviolet rays within 2.0 ± 0.3 ns, which was short enough compared to either the beam width of 50 ns or a multichannel-scalar dwell time of 16 ns. The flight time of a secondary ion was given by the duration between two detection times of photons emitted at the projectile incidence on the target and of the secondary ion. Some of the ions incident on the target were scattered to the direction of the multipliers by the Rutherford scattering process and formed background in the TOF spectra. The spectra of the background caused by the scattered particles were measured without applying the extracting voltage and were subtracted from the TOF spectra.

The incident beam current was monitored by counting projectiles scattered to an angle of 60° with a solid state detector (SSD) during each measurement. A base and a working pressure were 5×10^{-7} and 3×10^{-6} Pa, respectively.

III. RESULTS AND DISCUSSION

A. Mass spectra of secondary ions

Figure 1 shows examples of the mass spectra of positively charged secondary-ion species for the InP, InAs, and InSb targets bombarded with 5.0-MeV Si^{3+} ions. These mass spectra were taken with the linear TOF spectrometer. The dominant species emitted from the In (group-V element) semiconductive compounds was In^+, and secondary atomic ions of the group V were scant. This fact shows the important role of surface ionization, whose probability depends on the ionization potential of each species, as shown in Table I, in producing secondary ions. The previous studies revealed that, as shown in Fig. 1, large cluster ions are produced abundantly from an insulating SiO_2 target, but are seldom emitted from a semiconductive Si target [4,5]. In the case of the In group-V semiconductive chemical compounds, large cluster ions were observed: $In_l^+ (l=2$ to 7) $In_lP_m^+ (l=1-9$ and $m=1-3)$, $In_lAs_m^+ (l=1-5$ and $m=1,2)$, and $In_lSb_m^+ (l=1-7$ and $m=1-4)$. The cluster ions produced from the In-V targets consist of only indium atoms or those attaching a few group-V atoms. For comparison, in the case of Ga-V semiconductive materials, in spite of intense Ga^+ ions emitted, cluster ions composed of only antimony atoms or those attaching a few Ga atoms are substantially emitted from GaSb, but cluster ions are hardly produced from GaP and GaAs [7–10].

B. Singly charged secondary atomic ions

As shown in Fig. 2, the yields of In^+, which is the dominant species emitted from the In-V semiconductive chemical compounds, depend scantly on the incident energy between 0.5 and 5.0 MeV, but the yields of the group-V atomic ions, which are minor components, increase with increasing projectile energy. The observed results are very similar to the case of GaP, GaAs, and GaSb [8]. The ionization potentials of the group-V atoms are much higher than those of the group-III atoms, as shown in Table I [16], and the different projectile-energy dependence of the yields of the group-III and -V atomic ions can be explained based on the surface

TABLE I. Properties of semiconductive materials [16].

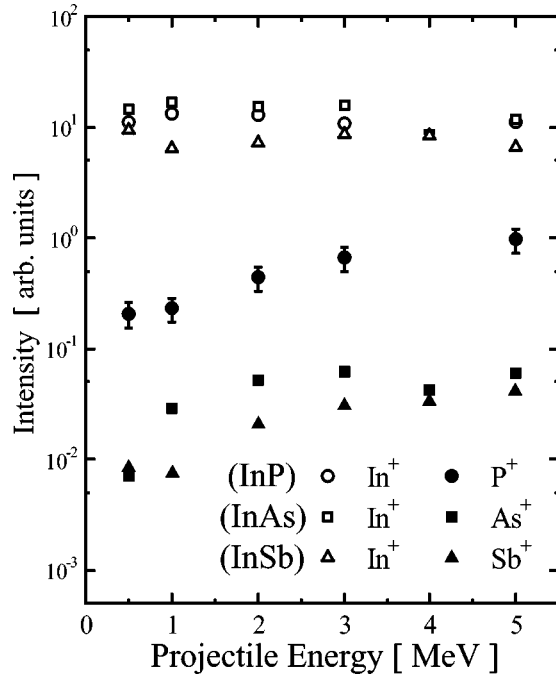| Type	Units	GaP	GaAs	GaSb	InP	InAs	InSb	Si
		N, undoped	N, Si doped	P, undoped	N, undoped	N, undoped	N, undoped	P, B doped
Min. energy gap (RT)[a]	eV	2.24	1.35	0.67	1.27	0.36	0.163	1.1
Electron mobility (RT)	$nm^2\ V^{-1}\ fs^{-1}$	30	880	400	460	3300	7800	190
Hole mobility (RT)	$nm^2\ V^{-1}\ fs^{-1}$	15	40	140	15	46	75	50
Ionization potential	eV		6.00 (Ga)			5.79 (In)		8.15
		10.5 (P)	9.79 (As)	8.61 (Sb)	10.5 (P)	9.79 (As)	8.61 (Sb)	

[a]RT=room temperature.

FIG. 2. Projectile-energy dependence of atomic ion yields.

ionization of the sputtered particles. Šroubek estimated the ionization probability P_e^+ of sputtered particles [17–19] by taking account of transient electronic excitation induced by ion bombardment and gave the formula

$$P_e^+ \propto \exp\left(-\frac{I - \varphi - \dfrac{e^2}{4v_\perp t_0}}{k_B T_{\text{eff}}}\right),\qquad(1)$$

where I is an ionization potential, φ a work function of a target, $v_\perp$ an axial emission velocity of an emitted atom, t_0 a relaxation time of the excited spot, e the electronic charge, k_B the Boltzmann constant, and T_{eff} an effective electron temperature. In the model, the ionization probability at the excited surface region increases effectively, because holes produced by the electronic excitation act as acceptors of electrons in the emitted atoms. This model successfully explains several cases of the low-energy ion-induced sputtering of metals [20,21]. The electronic excitation is characterized by T_{eff}, which correlates probably with the electronic stopping power S_e. The group-V secondary-atomic-ion yields relative to those of the corresponding group-III atomic ions are, then, plotted in Fig. 3 as a function of S_e^{-1}. Figure 3 shows that the atomic-ion yields depend exponentially on S_e^{-1} for all the III-V semiconductive compounds. This fact indicates that the projectile-energy dependence of the group-V atomic ions, as shown in Fig. 2, is caused by the increase of the ionization probability with increasing stopping power. The lifetime of the excited spot affecting the ionization probability depends on the mobilities of electrons and holes. For instance, as shown in Table I, the respective values for the InP target are 460 and 15 nm^2 V^{-1} fs^{-1} and are much lower than those for the InAs and InSb target. That is, the lifetime of the excited spot for the InP target is longer than those for
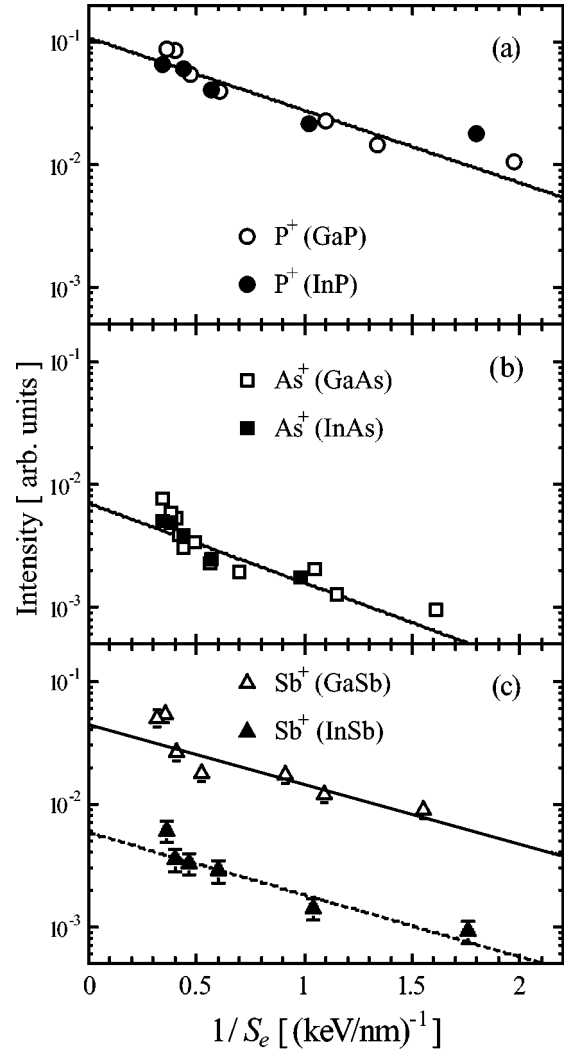

FIG. 3. S_e^{-1} dependence of the group-V secondary atomic ion yields relative to the corresponding In$^+$-ion yields. The dependence is also shown for the Ga-V targets [10]. The solid lines are drawn to guide the eye.

the other semiconductive compounds. As is evident from Figs. 2 and 3, the P$^+$ yield is really higher than those of As$^+$ and Sb$^+$, though the ionization potential of the P atom is higher than those of the As and Sb atoms. The low Sb$^+$ yield of InSb compared to that of GaSb can result from the very high mobility of electrons in InSb compared to that in GaSb.

Axial emission-energy distributions are shown in Fig. 4 for the P^{q+} (qe is the electric charge) and In$^+$ secondary ions. The distributions depend on neither the incident energy nor the target species. They have asymmetric shapes with gentle declines beyond the peaks. As shown in Fig. 4, the Sigmund-Thompson linear collision cascade model [22] can successfully reproduce the measured distributions of the singly charged secondary ions even at the MeV energy range by using reasonable surface potential energies, respectively.

C. Multiply charged secondary atomic ions

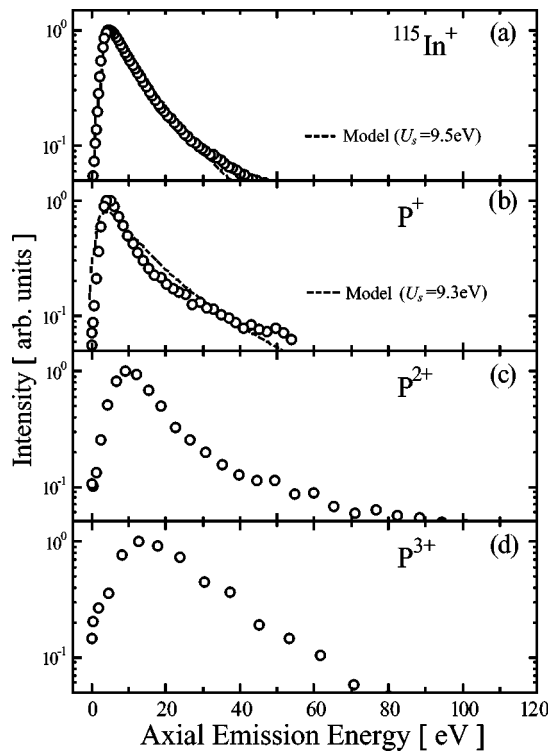Intense multiply charged P^{q+} ions were observed in the GaP [7] and InP cases. Figures 5 and 6 show, respectively,

FIG. 4. Axial emission-energy distributions for P^{q+} and In^+ secondary ions along with the expectations from the linear collision cascade theory.

the projectile-energy and electric-charge dependences of the P^{q+} yields relative to those of Ga^+ and In^+. The yields of Ga^+ and In^+ are almost independent of the projectile energy but those of P^{q+} increase with increasing projectile energy. The P^{q+} yields decrease slowly with the electric charge compared to the typical keV-energy cases; yield ratios of Si^{2+} to Si^{1+} and Ta^{2+} to Ta^{1+}, for example, are about 10^{-3} and 10^{-5}, respectively, and these results are explained by inner-shell excitations accompanied by the Auger-electron emission [23,24]. In addition, Fig. 4 shows that the emission energies of the multiply charged P^{q+} ions are higher than the corre-
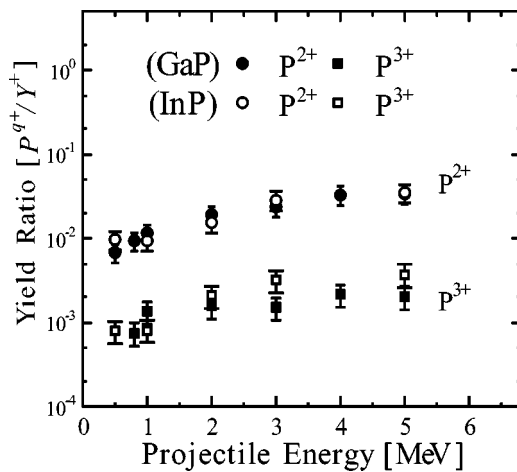

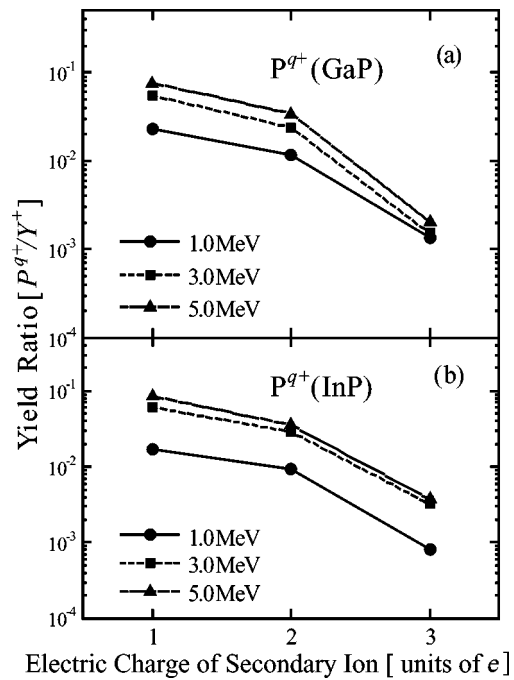FIG. 5. Projectile-energy dependence of the P^{q+} yields relative to those of Ga^+ and In^+.

FIG. 6. Electric-charge dependence of the P^{q+} yields relative to those of Ga^+ and In^+.

sponding values of the singly charged ions. This feature differs from the case of the multiply charged ions produced at the keV-energy incidence; in the latter case, the multiply charged ions are formed by the sequential process of the linear collision cascade and the Auger-electron emission outside the target and, consequently, have the same energy distributions as that of singly charged ions. The ionized track has a lifetime of 10^{-15}–10^{-14} s and is almost completely neutralized before the termination of the linear collision cascade. Multiply charged recoils produced by MeV-energy projectiles have very low energies and lose their charges by a collision with a target atom. These facts mean that no multiply charged ion can get out of the target through the linear collision cascade process lasting at least 10^{-13} s. Only multiply charged ions produced from the outermost atomic layer have any chances to be emitted. However, a projectile cannot recoil an atom to a backward direction and furthermore an ionized atom being accelerated by only the Coulomb repulsive force cannot get a kinetic energy enough to overcome a surface potential within 10^{-15}–10^{-14} s. Then, a candidate for the emission process of the multiply charged P^{q+} ions is a simultaneous process of ionization and recoiling of atoms constituting the outermost atomic layer by a single MeV-energy projectile [4]. That is, first, the formation cross section of a given multiply charged ion was found to be calculated on the basis of an independent-electron model [25–27]. Second, as shown in Fig. 7, the most probable and mean energies of the axial emission-energy distributions increase with increasing electric charge of the secondary ion. This feature can be explained as follows: When a target atom constituting the outermost atomic layer is recoiled at an angle close to $90°$ with a kinetic energy of a few eV and is ionized at the same time, the atom is accelerated further to the backward direction by the repulsive Coulomb force from
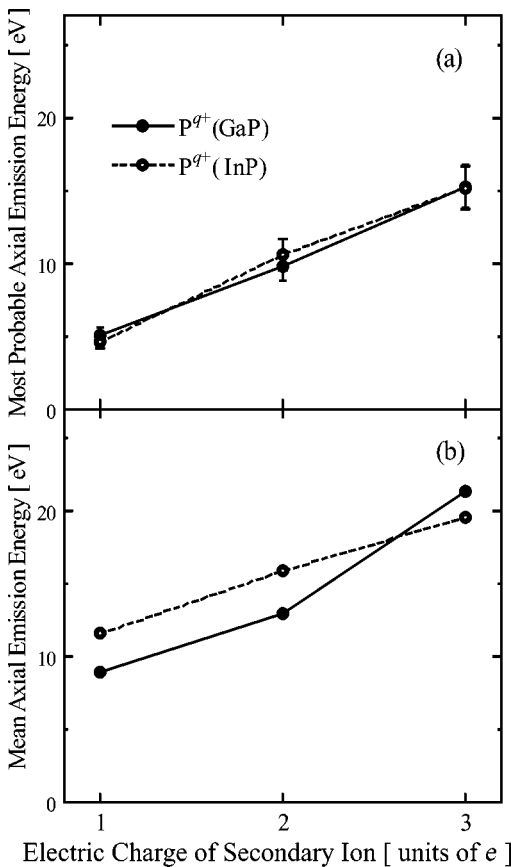
FIG. 7. Electric-charge dependence of the most probable and mean energies.

D. Secondary cluster ions

Figure 8 shows the relative secondary cluster-ion yields for the InP, InAs, and InSb targets as a function of projectile energy. These yields are shown relative to the corresponding yields of In^+, because the In^+ yields show the very weak dependence on the incident energy between 0.5 and 5.0 MeV. The yields of the group-V atomic ions and those of secondary ions emitted from the SiO_2 and Si targets are also plotted for comparison. The yields of In_2^+, In_3^+, and In_4^+ remain constant or decrease slightly with increasing incident energy; thus, they show dependences similar to those of In^+. On the other hand, the yields of InP^+, $InAs^+$, and In_3As^+ increase with increasing incident energy; hence, the results reflect the incident-energy dependences of the P^+, As^+, and Sb^+ yields. In the energy region studied, the yield of In_2^+ is independent of the incident energy or slightly decreases with incident energy. Because of a high ionization probability of In_2 caused by an expected low ionization potential, the total sputtering yields for the In group-V targets probably trace the dependence of In_2^+ on incident energy. By this reason, the total individual yields of clusters containing the elements in the group V from InP, InAs, and InSb are expected to scarcely depend on the incident energy between 0.5 and 5 MeV, too. In a manner similar to the singly charged group-V atoms, the yields of InP^+, $InAs^+$, and $InSb^=$ are plotted in Fig. 9 as a function of S_e^{-1} along with the cases of GaP^+ and $GaSb^+$. The results show the same dependence as found for the P^+, As^+, and Sb^+ yields. This means that the yields of cluster ions containing the group-V elements increase with increasing electronic stopping power because of the increase of the ionization probability caused by the transient electronic excitation induced by ion bombardment.

Figure 10 shows the cluster-size dependence of the cluster-ion yields for the InP, InAs, and InSb targets under 0.5, 3.0, and 5.0 MeV Si ion bombardment, along with the results of the GaSb and SiO_2 targets. The cluster-ion yields show the power-law dependence on the cluster size: $Y(n) \propto n^{-\delta}$. The obtained exponents δ are almost independent of

neighboring ionized target atoms in the track region and can overcome the surface potential within the life of the ionized track being 10^{-15}–10^{-14} s. The Coulomb repulsive energy is estimated to be about $(5-7) \times q$ eV on an average when the nearest lying atoms are assumed to be singly ionized on average.
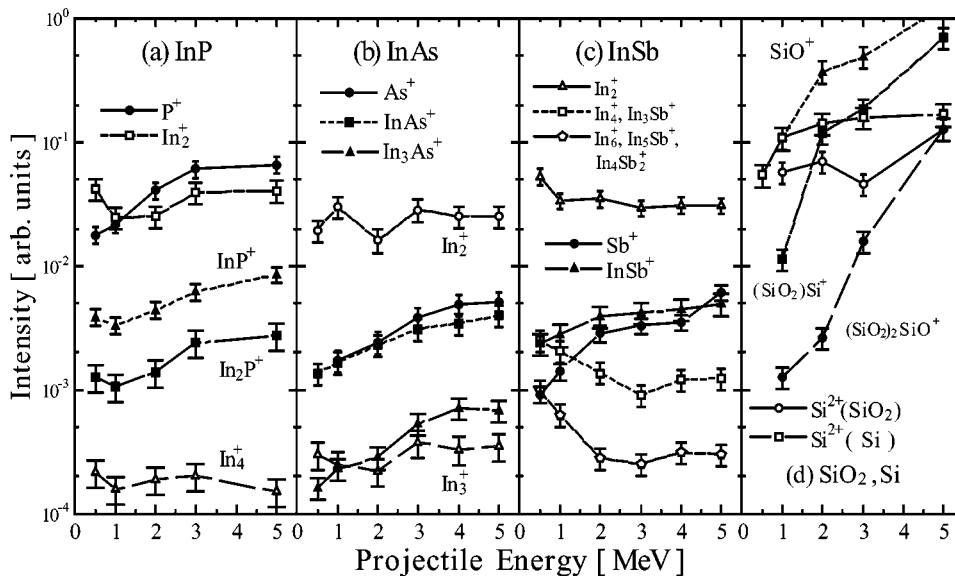

FIG. 8. Secondary-ion yields for the (a) InP, (b) InAs, and (c) InSb targets as a function of projectile energy. The yields of the secondary ions produced from the (d) SiO_2 and Si targets are also plotted [4,5].
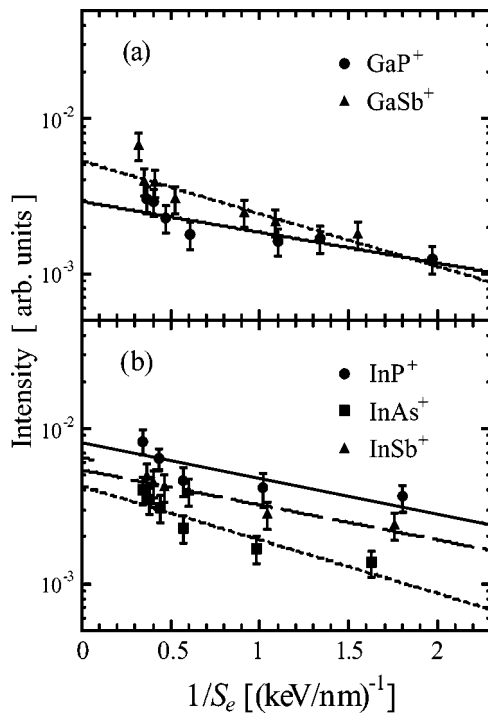
FIG. 9. S_e^{-1} dependence of the cluster ion yields emitted from the semiconductive chemical compounds.

the projectile energy and are 5.6–6.0 for the GaSb target, 3.7–3.8 for the InP target, 5.5–5.9 for the InAs target, and 5.1–5.4 for the InSb target. That is, the increase of the electronic stopping power does not affect the size distribution in the case of the III-V semiconductive materials. This electronic-stopping-power independence of δ is quite contrast to the drastic dependence for the SiO_2 target, where the observed exponents δ are 6.4 ($S_e=1.5$ keV nm^{-1}), 4.9 (3.5 keV nm^{-1}), and 3.4 (4.5 keV nm^{-1}). This difference of the electronic-stopping-power dependence of δ indicates that the sputtering mechanism of the semiconductive chemical compounds is different from that for the SiO_2 target. As described in a previous report [5], the yields of cluster ions emitted from the SiO_2 target are represented well by a simple power function of $Y=AS_e^B$. The exponent B increases with increasing mass of cluster ions. From these results, it was concluded that the cluster ions produced from the SiO_2 target are emitted directly through the multiple-bond-breaking process by secondary electrons [5,9]. Really in insulating materials the electronic excitation on the surface is sustained long enough to induce the multiple bond breaking. That is, Guizard *et al.* reported a value of free-carrier lifetime in SiO_2 to be 1.5×10^{-13} s [28]. Meftah *et al.* reported that an ion track is surely formed above a stopping power of 2 keV nm^{-1} for SiO_2 [29]. On the other hand, the lifetime in metals is estimated to be 10^{-16}–10^{-15} s, when it is assumed that the radius of the excited spot is $1–10$ nm and the velocity of the electron is about the Fermi velocity in metals. The lifetime is too short to induce the multiple bond breaking. So far, no measurement of the free-carrier lifetime and the ion track was reported for the semiconductive compounds, but it is surely longer than that of the metals and shorter than that
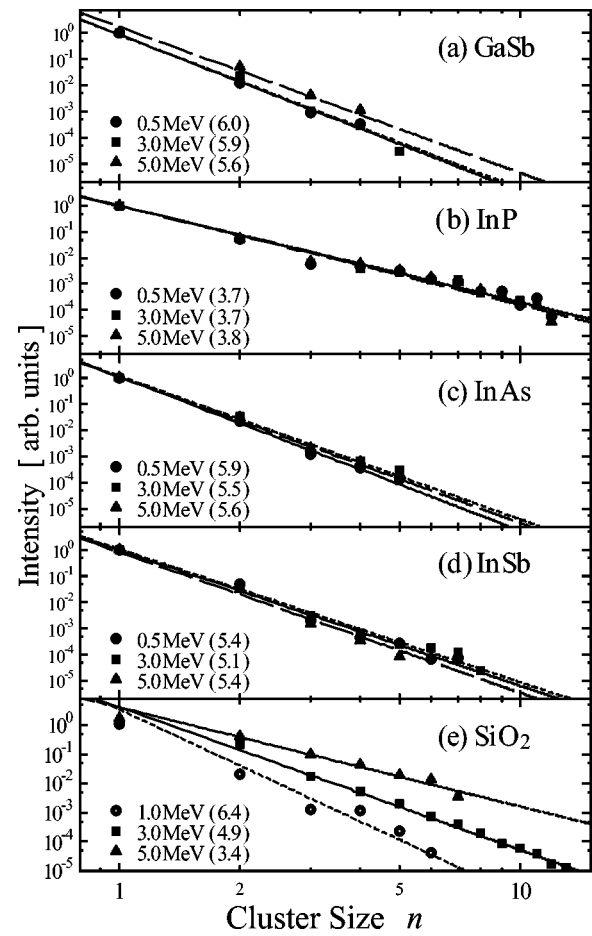

FIG. 10. Cluster-size dependence of the summed-up cluster-ion yields for the GaSb [9,10], InAs, InP, and InSb targets under 0.5 (circles), 3.0 (squares), and 5.0 (triangles) MeV Si ion bombardment. The straight lines show the power-law dependence. The cluster-ion yields are also plotted for the SiO_2 target under 1.0 (double circles), 3.0, and 5.0 MeV Si ion bombardment.

of the insulators. In the semiconductive compounds, broken bonds are possibly restored before the secondary cluster ions are emitted, because the secondary cluster ions are considered to be emitted in 10^{-13} s. Then, the multiple-bond-breaking process applied to SiO_2 cannot take place in the case of the semiconductive materials.

On the other hand, many studies have been recently done about the neutral- and charged-cluster emission under ion bombardment on noninsulating solids [30–34], though most of the experiments were limited to an ion bombardment less than several tens of keV. In these experiments, cluster yields have been found to have a power-law dependence on the cluster size [31–34], and in the case of a size smaller than about 20, the exponent δ has been found to correlate with the total sputtering yield, such that higher sputtering yields result in a smaller value of δ [31,32]. For instance, values of δ were reported to be 7.9 (Cu) and 9.3 (Al) by Coon *et al.* [31] and 3.3 to 3.7 (Ag), 6.7 (Cu), and 5.7 to 6.1 (In) by Wucher and co-workers [32–34]. For large clusters the value of δ has been found to be independent of the yield and is around 2 [34,36]. Only a few theoretical models predict the power-law size distribution of the cluster formation. The thermal equi-

librium model of Urbassek [35] and the shock-wave model of Bitensky and Parilis [14] predicted the power-law dependence. The values of δ predicted by these models are 2 and 7/3, respectively, and both the values agree with the results for the large clusters. In order to reproduce the large values of δ obtained for the small clusters, taking into account dissociation of nascent large clusters after emission, Wucher and Garrison [37] tried a molecular dynamics simulation using the many-body MD/MC-corrected effective medium potential developed by Stave et al. [38] and succeeded to qualitatively reproduce the experimental results. Meanwhile, a value of about 2 was obtained for the exponent in the case of small hydrogenated carbon clusters produced by highly charged ion impact on solid C_{84}. The result is not inconsistent with those of the metals because a large part of the deposited energy is probably consumed as an internal energy in a localized C_{84} and, in addition, emitted carbon clusters are less fragile than the metallic clusters.

In the case of MeV-projectile bombardment, the nuclear collision is not a dominant process at all. Therefore, it is difficult to directly apply the above models to the present case. However, Stampfli and Bennemann proposed that the diamond or zinc-blende structure of group IV (Si, Ge, and C) and group III-V (GaAs, etc.) becomes unstable against shear distortions in the presence of a sufficiently dense electron-hole plasma [39,40], and this lattice instability is considered to be a possible cause of multiple-charged ion-induced sputtering and laser ablation in GaAs [41–43]. In this model, when a considerable part of the valence electrons is excited into the conduction band, transverse acoustic phonons become instable, and strong anharmonic interactions subsequently affect longitudinal optical phonons. The energy gap between the conduction and the valence bands vanishes, resulting in metallic properties. The lattice instability causes atomic displacements of more than 0.1 nm and considerable kinetic energies of the atoms, which lead to very rapid melting of the crystal. Then, it is expected that large nascent clusters are emitted through a process similar to the thermal-equilibrium model or the shock-wave model. The large nascent clusters have high internal energies and result in the disintegration into small ionic clusters. In this case, the exponent should be larger than 2. Incidentally, cluster ions are observed in every In-V compound though only GaSb produces cluster ions among the Ga-V compounds. These results are expected because of the narrow gaps and the average large mass of the In-V compounds. That is, decrease of the band gap increases the percentage of electrons excited from the valence band, and the time t_i required for the instability depends on a bond length d and an average atomic mass M, and scales as $t_i \propto d^{-2} M^{-1/2}$.

IV. SUMMARY

When the In group-V semiconductive compounds were irradiated by Si ions with energies from 0.5 to 5.0 MeV, where the nuclear stopping power decreases with increasing projectile energy and vice versa for the electronic stopping power, various secondary ions such as large cluster ions and atomic ions were observed. The yields of the group-V atomic ions and the cluster ions containing the group-V atoms increase with increasing projectile energy, though those of the In atomic ions and the cluster ions composed of only In atoms keep constant or decrease slightly with increasing projectile energy. The yields of the ions containing the group-V elements can be expressed by an exponential function of S_e^{-1} for the In-V semiconductive compounds. The fact shows that the ionization probabilities of the atoms and the clusters whose ionization potentials are much higher than the work functions of target materials are increased by the transient electronic excitation induced by ion bombardment.

The energy distributions of atomic ions show that the singly charged atomic ions are emitted through the linear collision cascade process even at the MeV-energy range, and the multiply charged ions are produced through the projectile-induced simultaneous process of ionization and recoiling of atoms on the target surface.

The yield dependences on electronic stopping power and on cluster size are so much different between the chemical semiconductive materials and the insulator of SiO_2. The fact precludes the multiple-bond-breaking process applied to the insulating material. Structural instabilities caused by high-density electronic excitations, which are known to take place in GaAs irradiated by slow multiply charged ions or lasers, are also a possible cause of the cluster-ion emission from the semiconductive compounds at the MeV-energy range.

[1] D. F. Torgerson, R. P. Skowronski, and R. D. Macfarlane, Biochem. Biophys. Res. Commun. **60**, 616 (1974).

[2] R. E. Johnson and W. L. Brown, Nucl. Instrum. Methods Phys. Res. **198**, 103 (1982).

[3] B. U. R. Sundqvist, Nucl. Instrum. Methods Phys. Res. B **48**, 517 (1990).

[4] S. Kyoh, K. Takakuwa, M. Sakura, M. Umezawa, A. Itoh, and N. Imanishi, Phys. Rev. A **51**, 554 (1995).

[5] N. Imanishi, S. Kyoh, A Shimizu, M. Imai, and A Itoh, Nucl. Instrum. Methods Phys. Res. B **135**, 424 (1998).

[6] N. Imanishi, H. Ohta, S. Ninomiya, and A Itoh, Nucl. Instrum. Methods Phys. Res. B **164-165**, 803 (2000).

[7] S. Ninomiya, N. Imanishi, J. Xue, S. Gomi, and M. Imai, Nucl. Instrum. Methods Phys. Res. B **193**, 745 (2002).

[8] S. Ninomiya, S. Gomi, C. Imada, M. Nagai, M. Imai, and N. Imanishi, Nucl. Instrum. Methods Phys. Res. B **209**, 233 (2003).

[9] S. Ninomiya and N. Imanishi, Vacuum **73**, 79 (2004).

[10] N. Imanishi and S. Ninomiya, J. Nucl. Radiochem. Sci. **5**, R9 (2004).

[11] J. A. M. Pereira and E. F. da Silveira, Surf. Sci. **390**, 158 (1997).

[12] W. L. Brown, W. M. Augustyniak, E. Brody, B. Cooper, L. J. Lanzerotti, A. Ramirez, R. Evatt, and R. E. Johnson, Nucl. Instrum. Methods **170**, 321 (1980).

[13] L. E. Seiberling, J. E. Griffith, and T. A. Tombrello, Radiat. Eff. **52**, 201 (1980).

[14] I. S. Bitensky and E. S. Parilis, Nucl. Instrum. Methods Phys. Res. B **21**, 26 (2000).

[15] R. E. Johnson, B. U. R. Sundqvist, A. Hedin, and D. Fenyö, Phys. Rev. B **40**, 49 (1989).

[16] D. R. Lide, *CRC Handbook of Chemistry and Physics*, 81st ed. (CRC, Boca Raton, FL, 2000-2001).

[17] Z. Šroubek, Phys. Rev. B **25**, 6046 (1982).

[18] Z. Šroubek, Nucl. Instrum. Methods Phys. Res. **194**, 533 (1982).

[19] Z. Šroubek and J. Lörinčík, Vacuum **56**, 263 (2000).

[20] M. A. Karolewski and R. G. Gavell, Surf. Sci. **480**, 47 (2001).

[21] S. F. Belykh, I. A. Wojciechowski, V. V. Palitsin, A. V. Zinoviev, A. Adriaens, and F. Adams, Surf. Sci. **488**, 141 (2001).

[22] P. Sigmund, Phys. Rev. **184**, 383 (1969).

[23] J. Maul and K. Wittmaack, Surf. Sci. **47**, 358 (1975).

[24] K. Wittmaack, Surf. Sci. **53**, 626 (1975).

[25] R. E. Olson, J. Phys. B **12**, 1843 (1979).

[26] J. Ullrich, K. Bethge, S. Kelbch, W. Schadt, H. Schmidt-Böking, and K. E. Stiebing, J. Phys. B **19**, 437 (1986).

[27] H. Tawara, T. Tonuma, H. Kumagai, and T. Matsuo, Phys. Rev. A **41**, 116 (1990).

[28] S. Guizard, P. Martin, Ph. Daguzan, G. Petite, P. Audebert, J. P. Geindre, A. Dos Santos, and A. Antonnetti, Europhys. Lett. **29**, 401 (1995).

[29] A. Meftah, F. Brisard, J. M. Costantini, M. Hage-Ali, J. P. Stoquert, F. Studer, and M. Toulemonde, Phys. Rev. B **48**, 920 (1993).

[30] I. Katakuse, T. Ichikawa, Y. Fujita, T. Matsuo, T. Sakurai, and H. Matsuda, Int. J. Mass Spectrom. Ion Processes **74** 33 (1986).

[31] S. R. Coon, W. F. Calaway, J. W. Burnett, M. J. Pellin, D. M. Gruen, D. R. Spiegel, and J. M. White, Surf. Sci. **259**, 275 (1991).

[32] A. Wucher and M. Wahl, Nucl. Instrum. Methods Phys. Res. B **115**, 581 (1996).

[33] Th. J. Colla, H. M. Urbassek, A. Wucher, C. Staudt, R. Heinrich, B. J. Garrison, C. Dandachi, and G. Betz, Nucl. Instrum. Methods Phys. Res. B **143**, 284 (1998).

[34] C. Staudt and A. Wucher, Phys. Rev. B **66**, 075419 (2002).

[35] H. M. Urbassek, Nucl. Instrum. Methods Phys. Res. B **31**, 541 (1988).

[36] L. E. Rehn, R. C. Birtcher, S. E. Donnelly, P. M. Baldo, and L. Funk, Phys. Rev. Lett. **87**, 207601 (2001).

[37] A. Wucher and B. J. Garrison, J. Chem. Phys. **105**, 5999 (1996).

[38] M. S. Stave, D. E. Sanders, T. J. Raeker, and A. E. DePristo, J. Chem. Phys. **93**, 4413 (1990).

[39] P. Stampfli and K. H. Bennemann, Phys. Rev. B **49**, 7299 (1994).

[40] P. Stampfli, Nucl. Instrum. Methods Phys. Res. B **107**, 138 (1996).

[41] T. Schenkel, A. V. Hamza, A. V. Barnes, D. H. Schneider, J. C. Banks, and B. L. Doyle, Phys. Rev. Lett. **81**, 2590 (1998).

[42] T. Schenkel, A. V. Hamza, A. V. Barnes, and D. H. Schneider, Prog. Surf. Sci. **61**, 23 (1999).

[43] L. Huang, J. P. Callan, E. N. Glezer, and E. Mazur, Phys. Rev. Lett. **80**, 185 (1998).